



Diffusion of dilute gas in arrays of randomly distributed, vertically aligned, high-aspect-ratio cylinders

Wojciech Szmyt^{*1,2,3}, Carlos Guerra¹ and Ivo Utke^{*1}

Full Research Paper

Open Access

Address:

¹Empa, Swiss Federal Laboratories for Materials Science and Technology, Laboratory for Mechanics of Materials and Nanostructures, Feuerwerkerstrasse 39, 3602 Thun, Switzerland, ²AGH University of Science and Technology, Faculty of Physics and Applied Computer Science, al. A. Mickiewicza 30, 30-059 Krakow, Poland and ³now working at: FHNW University of Applied Sciences and Arts Northwestern Switzerland, Institute of Polymer Engineering, Klosterzelgstrasse 2, 5210 Windisch, Switzerland

Email:

Wojciech Szmyt^{*} - wojciech.szmyt@fhnw.ch;
Ivo Utke^{*} - ivo.utke@empa.ch

* Corresponding author

Keywords:

dilute gas; gas transport; molecular diffusion; nanocylinders; random walk

Beilstein J. Nanotechnol. **2017**, *8*, 64–73.

doi:10.3762/bjnano.8.7

Received: 11 August 2016

Accepted: 13 December 2016

Published: 09 January 2017

Associate Editor: P. Ziemann

© 2017 Szmyt et al.; licensee Beilstein-Institut.

License and terms: see end of document.

Abstract

In this work we modelled the diffusive transport of a dilute gas along arrays of randomly distributed, vertically aligned nanocylinders (nanotubes or nanowires) as opposed to gas diffusion in long pores, which is described by the well-known Knudsen theory. Analytical expressions for (i) the gas diffusion coefficient inside such arrays, (ii) the time between collisions of molecules with the nanocylinder walls (mean time of flight), (iii) the surface impingement rate, and (iv) the Knudsen number of such a system were rigidly derived based on a random-walk model of a molecule that undergoes memoryless, diffusive reflections from nanocylinder walls assuming the molecular regime of gas transport. It can be specifically shown that the gas diffusion coefficient inside such arrays is inversely proportional to the areal density of cylinders and their mean diameter. An example calculation of a diffusion coefficient is delivered for a system of titanium isopropoxide molecules diffusing between vertically aligned carbon nanotubes. Our findings are important for the correct modelling and optimisation of gas-based deposition techniques, such as atomic layer deposition or chemical vapour deposition, frequently used for surface functionalisation of high-aspect-ratio nanocylinder arrays in solar cells and energy storage applications. Furthermore, gas sensing devices with high-aspect-ratio nanocylinder arrays and the growth of vertically aligned carbon nanotubes need the fundamental understanding and precise modelling of gas transport to optimise such processes.

Introduction

Arrays of vertically aligned nanowires and nanotubes with high-aspect ratio composed of various materials have been widely used in science and industry. Arrays of silicon nanowires [1,2] and carbon nanotubes [3] are undoubtedly the most popular high-aspect-ratio cylinder array systems. Moreover, there has been growing interest in nanocylinder systems composed of metals [4], and metal oxides [5,6] have become increasingly researched for their use as large-surface one-dimensional materials in a wide range of potential fields of applications such as photovoltaics [7], photocatalysis [8], organic electronics [9] and supercapacitors [10].

Surface functionalisation and nanoengineering of high-aspect-ratio nanocylinder arrays often involve the exposure of the structures to gas-phase chemicals, for instance, during the coating of nanotubes or nanowires with thin films employing techniques such as chemical vapour deposition (CVD) [11] or atomic layer deposition (ALD) [12,13]. Our recent study constitutes an example of the coating of vertically aligned carbon nanotubes (VACNTs) with monocrystalline anatase using ALD [14]. Arrays of nanocylinders are also used in gas sensing systems [15,16]. The increasing interest in surface functionalisation via gas phase techniques as well as gas sensing applications with high-aspect-ratio nanocylinder arrays has raised the need for the fundamental understanding and precise modelling of gas-transport specifics required in the optimisation of the aforementioned processes [17]. Furthermore, root growth of VACNTs with a CVD method has been reported to be limited by gas diffusion, which additionally emphasizes the need for a reliable method of gas-transport modelling [18,19]. The understanding of the gas-transport kinetics within nanocylinder arrays will be also crucial in the design and optimisation of the industrially up-scalable spatial ALD processes [20] carried out on such substrates. Although processes based on gas transport in various types of nanocylinder arrays have been extensively studied for years, rather less attention has been paid to modelling of the diffusion phenomena. Diffusion modelling was attempted in the context of ALD coatings of CNTs [17] or VACNT growth [19,21,22]. These studies deliver rough estimates of the gas transport and lack rigidly derived formulae of gas diffusion inside a nanocylinder array. Most studies have been so far devoted to gas transport within more classic porous structures such as narrow holes or trenches constituting a foundation of the considerations of this study. The theory of molecular diffusion across nanopores has been developed by Martin Knudsen more than a century ago [23,24]. Knudsen's theory handles surface collisions of molecules by diffusive reflection (following Lambert's cosine law) and neglects specular reflection. It has been successfully and widely tested for microchannels and nanopores [25,26], as well as for ALD growth in

nanopores [27-31], and conformal CVD [32] considering kinetic parameters of surface sticking, surface diffusion, adsorption and desorption phenomena as a function of gas pressure and temperature. Recently Arya et al. [33,34] suggested that for atomically smooth surfaces specular reflection may contribute to surface diffusion. While for pristine and uncoated CNT arrays and certain gas molecules this may be the case, it seems that the ALD coating process is simulated by diffusive reflection [27,28]. Here, we derive gas-transport formulae based on diffusive reflection in randomly distributed vertically aligned arrays of nanocylinders (nanotubes or nanowires). We would like to point out that our approach can also be used to derive expressions for diffusion accounting for specular reflections.

We present rigid derivations of the gas diffusion coefficient D inside such arrays, the time between collisions of molecules with nanocylinder walls, τ , the molecule surface impingement rate, J , and the Knudsen number of such a system, Kn . The derivations have been performed employing a random-walk model of gas molecules undergoing memoryless, diffusive reflection from nanocylinder walls assuming the molecular regime of gas transport. The example calculation of a diffusion coefficient is delivered for a system of titanium isopropoxide molecules diffusing between vertically aligned carbon nanotubes coated with titanium dioxide, which is especially relevant for applications in ALD.

Foundations of the developed model

Physical assumptions

We use the following assumptions for the gas-transport conditions within the model system of nanocylinders:

- The gas is dilute, meaning that intermolecular collisions can be neglected and within the space confined by nanocylinders the diffusion occurs in a molecular regime.
- The system of nanocylinders is of high aspect ratio, which from the point of view of diffusion means a large ratio of cylinder length to mean horizontal penetration depth.
- The system exhibits a continuous translational symmetry in transverse direction owing to the random cylinder distribution on the substrate surface, which allows us to reduce the three-dimensional diffusion problem to one dimension along the tube axis.
- Lambert's cosine law is assumed for memoryless, diffusive re-emission (reflection) of gas molecules from the nanocylinder surface.

For the sake of clarity, dimensions of a molecule are assumed much smaller than both the nanocylinder diameter and the flight

distance of the molecules. The finite molecular dimension can be taken into account by extending the parameter of nanocylinder diameter d with the molecular diameter d_m resulting in $\tilde{d} = d + d_m$. The model system is schematically illustrated in Figure 1.

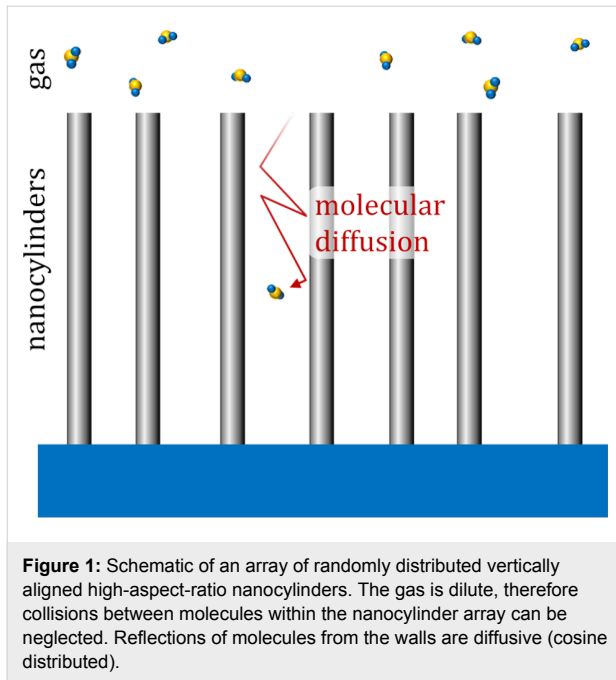


Figure 1: Schematic of an array of randomly distributed vertically aligned high-aspect-ratio nanocylinders. The gas is dilute, therefore collisions between molecules within the nanocylinder array can be neglected. Reflections of molecules from the walls are diffusive (cosine distributed).

In the derivations we have employed a random-walk model of a molecule being diffusively reflected from the nanocylinder walls. Provided that there is no correlation between subsequent random-walk steps, according to the Einstein–Smoluchowski approach [35], the diffusion coefficient can be expressed as

$$D = \frac{\lambda^2}{2k\tau}, \quad (1)$$

where λ^2 is the mean square displacement, τ is the mean time of flight between two successive wall collisions and k is the number of dimensions in which the diffusion occurs. Attenuation of the molecule flux into the array by molecules hitting the top faces of the cylinders does not require consideration because the variable describing the diffusing species is solely the concentration of molecules within the volume of space unoccupied by obstacles.

Definition of the system geometry

The geometry of a nanocylinder array is defined by the nanocylinder areal density, σ , and the mean nanocylinder diameter, d , as shown in Figure 2. The figure illustrates a mean number of nanocylinders $\langle \Delta N \rangle$ on a given substrate area ΔS , which can be estimated as the product of ΔS and σ .

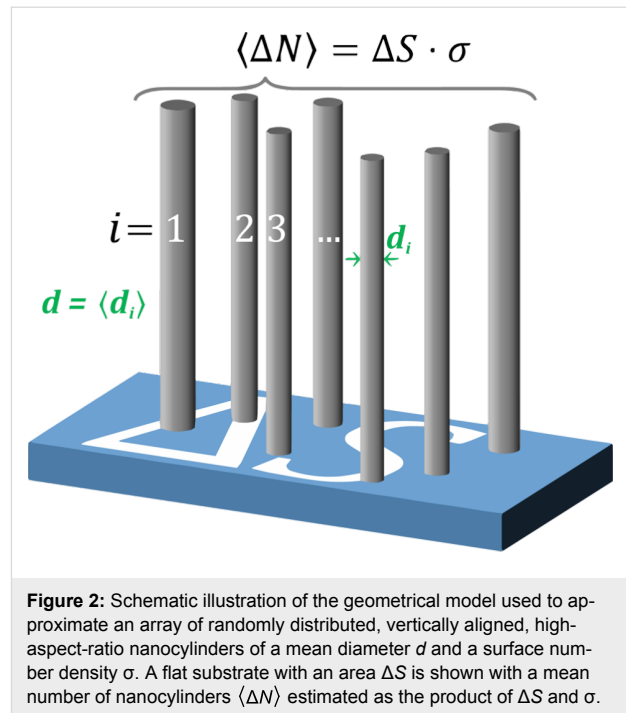


Figure 2: Schematic illustration of the geometrical model used to approximate an array of randomly distributed, vertically aligned, high-aspect-ratio nanocylinders of a mean diameter d and a surface number density σ . A flat substrate with an area ΔS is shown with a mean number of nanocylinders $\langle \Delta N \rangle$ estimated as the product of ΔS and σ .

Results and Discussion

In this chapter we present derivations that emerge from the definitions and assumptions given above. In order to fully describe the kinematics of molecular diffusion, we deliver physical formulae describing i) the mean time of flight of a diffusant, τ , ii) the cylinder wall impingement rate, J , and iii) the diffusion coefficient, D . Additionally, we derive the Knudsen number Kn and define a gas-transport aspect ratio AR_{array} , which allow us to assess whether the assumptions of molecular diffusion and high aspect ratio are justified in the given system and deliver an example calculation for a system that was proven to fulfil both assumptions. To initiate the random-walk approach, we describe the probability distributions of the transverse penetration distance, x , and a diffusive reflection angle θ , which will serve as the basis of the further derivations.

Probability distribution of the transverse penetration distance

Although the molecules travel in all three dimensions, the flight distance of a molecule is confined by the distance at which it hits another tube wall in transverse direction, as the tubes are assumed long and vertical. The distance travelled in the transverse direction by a molecule diffusing through the array of nanocylinders will be denoted as x . From a point of view of a lateral flux of molecules, I , the nanocylinders act as tall targets of width d and lateral areal density σ . Thus, the flux I is attenuated across the infinitesimal distance dx by a factor equal to a fraction of the transverse projection unoccupied by the cylinders, as shown in Figure 3.

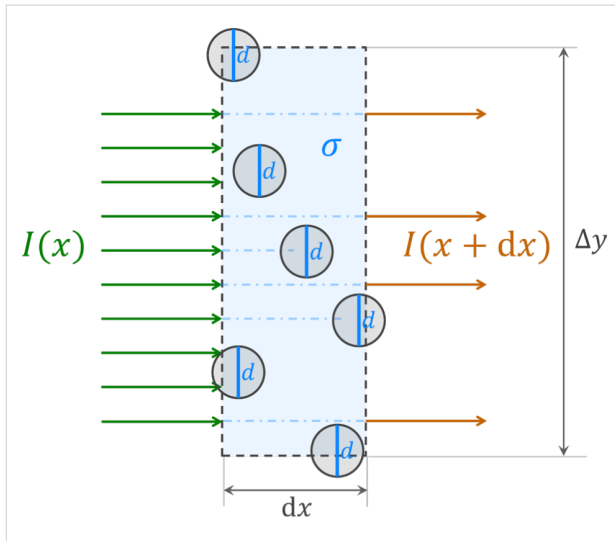


Figure 3: Top view schematic of the attenuation of a transverse flux I of molecules through the slice of a nanocylinder array of lateral dimensions $\Delta x \times \Delta y$. For clarity, the diameters in the figure were kept constant instead of randomly distributed, which does not alter the result of the derivation.

The attenuation factor is equivalent to the probability of transmission through a slice of thickness dx denoted as T_{dx} .

$$T_{dx} = 1 - \frac{\Delta N \cdot d}{\Delta y} = 1 - \frac{\Delta S \sigma \cdot d}{\Delta y} \quad (2)$$

$$= 1 - dx \cdot \sigma d = 1 - \frac{dx}{\lambda_T},$$

$$\lambda_T := \frac{1}{\sigma d}, \quad (3)$$

where the mean transverse penetration distance, λ_T , is implicitly defined. Note that the above reasoning is sensitive solely to the mean value of d and not to the specific form of the diameter distribution. We can derive the transverse flux transmitted through a slice of the cross-section of a finite thickness x , obtaining a differential equation and its solution:

$$T_{dx} \cdot I(x) = I(x + dx) = \left(1 - \frac{dx}{\lambda_T}\right) I(x) \quad (4)$$

$$\Rightarrow \frac{dI(x)}{dx} = -\frac{I(x)}{\lambda_T},$$

$$I(x) = I_0 e^{-\frac{x}{\lambda_T}}. \quad (5)$$

where $I(x = 0) = I_0$ has been placed as an initial condition. Knowing that the penetration distance probability density func-

tion $p(x)$ is proportional to the transmitted flux, we can obtain it by normalising the expression

$$p(x) = \frac{I(x)}{\int_0^\infty I(x) dx} = \frac{1}{\lambda_T} e^{-\frac{x}{\lambda_T}}. \quad (6)$$

The probability density function is exponential, meaning that the described process is Poissonian. In a recent study the expression

$$D = \frac{v}{3} d_{\text{equiv}}, \quad (7)$$

$$d_{\text{equiv}} = \left(\frac{1}{\sqrt{\sigma}} - d \right) \quad (8)$$

has been used as a pragmatic estimation of a lower limit of D in an array of vertically aligned carbon nanotubes [17], which constitutes an analogy to Knudsen diffusivity through cylindrical pores with the equivalent pore diameter designated as d_{equiv} . The limit of this approach is illustrated with an example geometry in Figure 4 using a mean spacing of nanocylinders of $1/\sqrt{\sigma} = 100$ nm ($\sigma = 10^{10}$ cm $^{-2}$) and a mean cylinder diameter of 25 ± 6 nm as an example. It is evident, that the lower-limit

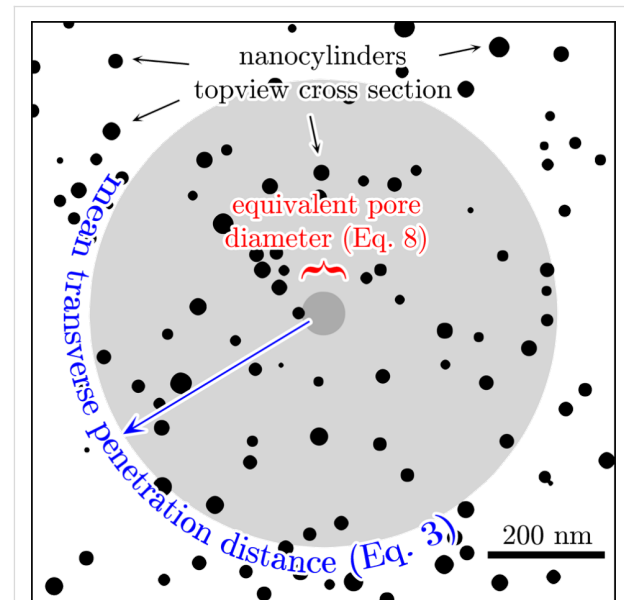


Figure 4: Illustration of the equivalent pore diameter (Equation 8) and the mean transverse penetration distance calculated using Equation 3. Diameters of nanocylinders are normally distributed with a mean value of 25 nm and a standard deviation of 6 nm. The nanocylinders are uniformly distributed on the substrate with an areal density of 10^{10} cm $^{-2}$.

guess strongly underestimates the mean transverse penetration distance. In the following we will develop the diffusion model towards a greater physical accuracy.

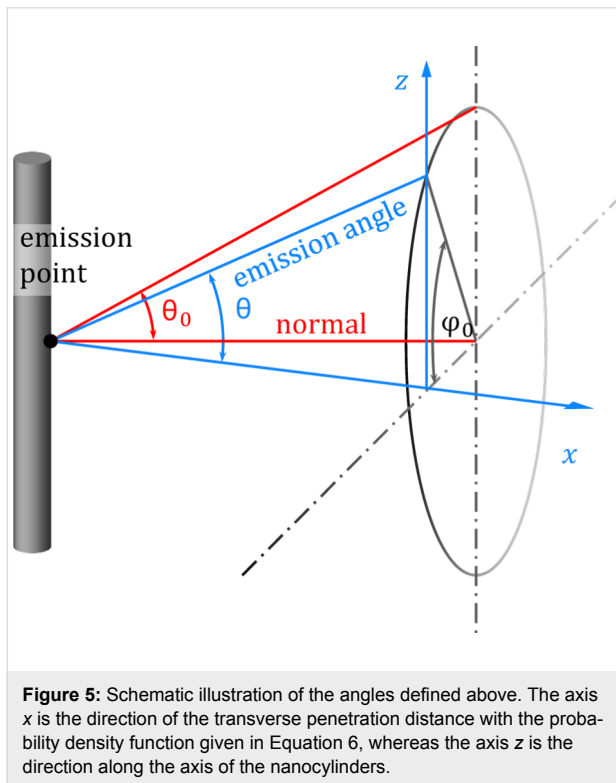
Angular distributions of diffusive reflection

As mentioned in the assumptions above, the collisions of molecules with the nanocylinder walls are memoryless and diffusive, meaning that the solid angle of re-emission after a collision is governed by Lambert's cosine law, independent of the angle of incidence [24,36]. The angle θ_0 measured with respect to the normal, and the azimuthal angle φ_0 have probability distribution functions given by

$$g(\theta_0) := \sin 2\theta_0, \theta_0 \in \left[0, \frac{\pi}{2}\right), \quad (9)$$

$$h(\varphi_0) := \frac{1}{2\pi}, \varphi_0 \in [0, 2\pi) \quad (10)$$

and they are independent of each other. The angles are visualized in Figure 5.



Considering the displacement of a molecule in the vertical direction along the axis of the nanocylinder, the only angle that is explicitly significant to the phenomenon is the angle in the vertical plane θ , which fulfils the condition

$$\sin \theta = \sin \theta_0 \sin \varphi_0. \quad (11)$$

Introducing a set of temporary variables (u , w and q) and their probability distribution functions denoted as “pdf” with the according subscripts

$$u := \sin \theta_0, u \in [0, 1) \quad (12)$$

$$\begin{aligned} \Rightarrow g(\theta_0) d\theta_0 &= \sin 2\theta_0 d\theta_0 \\ &= 2u du = \text{pdf}_u(u) du, \end{aligned} \quad (13)$$

$$w := \sin \varphi_0, w \in [-1, 1] \quad (14)$$

$$\begin{aligned} \Rightarrow h(\varphi_0) d\varphi_0 &= \frac{d\varphi_0}{2\pi} \\ &= \frac{dw}{2\pi\sqrt{1-w^2}} = \text{pdf}_w(w) dw, \end{aligned} \quad (15)$$

$$q := uw = \sin \theta, q \in (-1, 1), \quad (16)$$

we can obtain the probability density function of q being a product of two independent random variables u and w :

$$\begin{aligned} \text{pdf}_q(q) &= \int_q^1 \frac{1}{|u|} \text{pdf}_{u,w}\left(u, \frac{q}{u}\right) du \\ &= \int_q^1 \frac{1}{|u|} \text{pdf}_u(u) \text{pdf}_w\left(\frac{q}{u}\right) du \\ &= \int_q^1 \frac{1}{u} 2u \frac{1}{2\pi\sqrt{1-\left(\frac{q}{u}\right)^2}} du = \frac{2}{\pi} \sqrt{1-q^2}. \end{aligned} \quad (17)$$

The integration limits are taken to be q and 1, while from Equations 12–16 it is evident that u is always greater than q and the maximum value of u is 1. Accordingly, we obtain

$$\begin{aligned} \text{pdf}_q(q) dq &= \frac{2}{\pi} \sqrt{1-q^2} dq \\ &= \frac{2}{\pi} \cos^2 \theta d\theta = f(\theta) d\theta, \end{aligned} \quad (18)$$

$$f(\theta) := \frac{2}{\pi} \cos^2 \theta, \theta \in \left[-\frac{\pi}{2}, \frac{\pi}{2}\right). \quad (19)$$

Thus, we have obtained the probability density function f of the vertical emission angle θ , which is necessary for the further derivations.

Mean time of flight

Once the probability density functions are available, the time of flight can be derived. Knowing the transverse flight distance x and the angle in the vertical plane θ we calculate the flight distance:

$$\Delta s = \frac{x}{\cos \theta}. \quad (20)$$

Equation 20 is geometrically implied in Figure 6. To obtain the mean value of Δs a two-dimensional probability density function for both random variables x and θ is required. The variables are independent, therefore the distribution is the product of the two individual distributions:

$$\begin{aligned} \lambda_C &:= \langle \Delta s \rangle \\ &= \int_{-\pi/2}^{\pi/2} d\theta \int_0^{\infty} dx \Delta s(x, \theta) p(x) f(\theta) = \frac{4}{\pi} \lambda_T, \end{aligned} \quad (21)$$

where the mean confined flight path λ_C has been defined. The mean time of flight is therefore equal to

$$\tau = \frac{\lambda_C}{v} = \frac{4}{\pi v} \lambda_T. \quad (22)$$

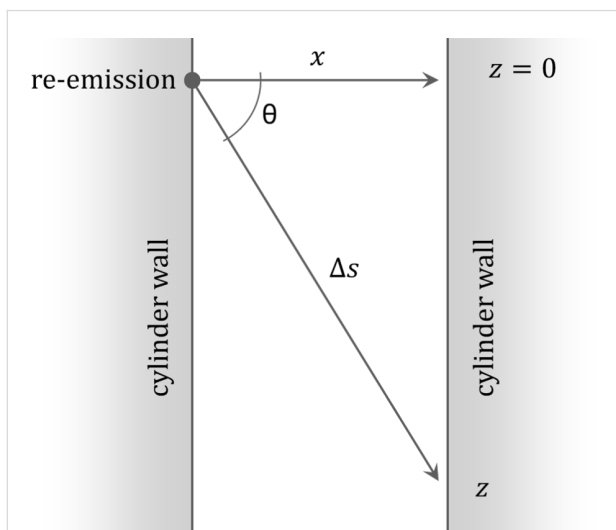


Figure 6: Schematic illustration of the flight geometry between two subsequent collisions of the molecule with a nanocylinder wall. The quantities in the figure are explained in the main text.

The velocity v can be taken as the mean absolute velocity from the Maxwell–Boltzmann distribution.

Impingement rate

The mean time of flight τ can be translated to the more commonly used impingement rate J by definition from gas kinetic theory:

$$\begin{aligned} J &= \frac{1}{\tau} \cdot \frac{\Delta N_m}{\Delta A} = \frac{1}{\tau} \cdot \frac{n \Delta V_v}{\Delta N \cdot \pi d \Delta z} \\ &= \frac{n}{\tau} \cdot \frac{\Delta z \Delta S - \Delta z \cdot \Delta N \frac{\pi d^2}{4}}{\Delta N \cdot \pi d \Delta z} \\ &= \frac{1}{\tau} \cdot \frac{\pi d^2}{\pi d} \\ &= \frac{n}{\tau} \frac{\sigma}{\pi d} \\ &= \frac{1}{4} n v \left(1 - \sigma \frac{\pi d^2}{4} \right), \end{aligned} \quad (23)$$

where ΔN_m refers to a number of molecules in an arbitrary volume within the nanocylinder array, ΔA is the area of nanocylinder walls in the given volume, n is the number volume density of molecules in the gas phase, whereas ΔV_v is the void volume between nanocylinders. The quantity $\sigma \pi d^2/4$ reflects the volume fraction occupied by the nanocylinders.

Diffusion coefficient

At this point, the only quantity that is yet to be derived to fully express D is the mean square displacement in the longitudinal direction λ^2 . It can be obtained as the mean value of z^2 . We deduce the longitudinal displacement in one flight z from the geometry in Figure 6:

$$z = x \tan \theta, \quad (24)$$

and derive λ^2 :

$$\begin{aligned} \lambda^2 &= \langle z^2 \rangle \\ &= \int_{-\pi/2}^{\pi/2} d\theta \int_0^{\infty} dx z^2(x, \theta) p(x) f(\theta) = 2\lambda_T^2. \end{aligned} \quad (25)$$

Using Equation 1, substituting τ obtained earlier and setting $k = 1$ as we consider only the longitudinal displacements, we can derive the equation for the diffusion coefficient D of gas molecules along an array of randomly distributed, vertically aligned, high-aspect-ratio cylinders:

$$D = \frac{\lambda^2}{2\tau} = \frac{\pi v}{4} \lambda_T = \frac{\pi v}{4} \frac{1}{\sigma d}. \quad (26)$$

It is to be noted that the mean square transverse displacement is equal to the mean square longitudinal displacement

$$\langle x^2 \rangle = \int_0^\infty x^2 p(x) = 2\lambda_T^2 = z^2. \quad (27)$$

However, the diffusion coefficient in transverse direction D_T is different from the one in longitudinal direction. Laterally, the diffusion is two-dimensional ($k = 2$). Therefore it is equal to

$$D_T = \frac{x^2}{2k\tau} = \frac{\pi v}{8} \frac{1}{\sigma d}, \quad (28)$$

which is half the value of the longitudinal one, and, effectively, the diffusion is anisotropic. The anisotropic diffusion is modelled with the three-dimensional diffusion equation

$$\frac{\partial n}{\partial t} = \nabla^T \mathbf{D} \nabla n, \quad (29)$$

where t is time, ∇ is the gradient column vector operator, the superscript “T” means transposition and \mathbf{D} is the diffusion matrix. In our case, \mathbf{D} takes the form

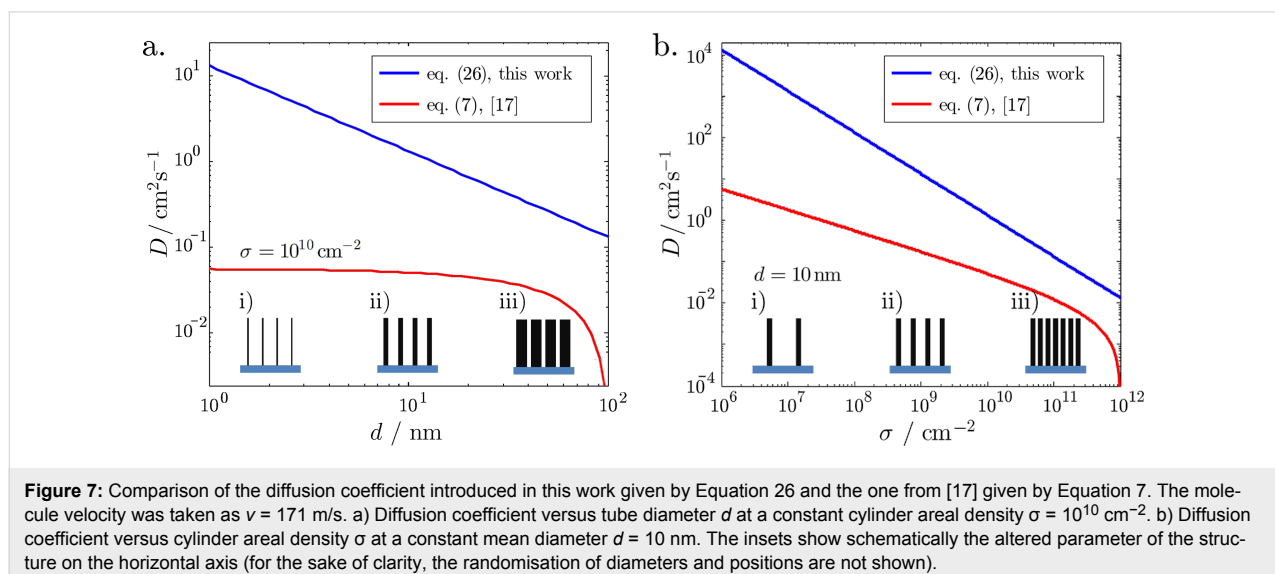
$$\mathbf{D} = \begin{pmatrix} 1/2 & 0 & 0 \\ 0 & 1/2 & 0 \\ 0 & 0 & 1 \end{pmatrix} \frac{\pi v}{4} \frac{1}{\sigma d}. \quad (30)$$

The off-diagonal terms in Equation 30 vanish because of the lacking correlation between the random motions of every pair of principal directions due to the random distribution of the vertical cylinders. The diffusion exhibits continuous translational and rotational symmetry around the direction of the cylinder axis. This would be violated by any correlation between the principal directions.

In the next part we compare Equation 26 with the lower limit expression in Equation 7. The comparison of the two diffusion coefficients is shown in Figure 7. In the calculations, titanium tetraisopropoxide (TTIP), which is a widely used gas precursor in ALD of titanium oxide [37], was taken as an example. The molecular weight of the compound is $M = 284.215$ g/mol. The temperature was taken to be $T = 100$ °C. Taking the expression for the mean absolute value of velocity from a Maxwell–Boltzmann distribution of molecule velocities from the classical kinetic theory of gas, one obtains

$$v = \sqrt{\frac{8RT}{\pi M}} = 171 \frac{\text{m}}{\text{s}}. \quad (31)$$

Numerical values of the diffusion coefficient using $v = 171$ m/s and Equation 26 are shown in Figure 7. In Figure 7a the areal density of nanocylinders $\sigma = 10^{10}$ cm⁻² was considered as an example of a high density of VACNTs grown by means of CVD [38] – the distance between the nanotubes then being estimated to be $\approx 1/\sqrt{\sigma} = 100$ nm. The diffusion coefficients are compared within a range of nanocylinder diameters from 1 to 100 nm. Analogously, in Figure 7b, the coefficients are compared at a constant diameter of 10 nm, with varying areal density from 10^6 to 10^{12} cm⁻².



The two formulas result in qualitatively different estimations of D . The effective pore diameter approach from [17] (Equation 7) would strongly underestimate the diffusion coefficient within the entire range of the tested parameters.

Knudsen number in an array of vertical randomly distributed nanocylinders

The molecular gas transport regime requires the mean flight path of molecules in a confined space λ_C to be much smaller than the mean free path in bulk gas λ_B at the same pressure and temperature. This condition implies that intermolecular collisions occur much less frequently than molecule–wall collisions, and consequently, their influence can be neglected. The ratio between λ_B and λ_C is called the Knudsen number

$$\text{Kn} := \frac{\lambda_B}{\lambda_C}, \quad (32)$$

and its magnitude allows us to assess whether the gas transport occurs in the molecular regime. Conventionally, the regime is molecular, when Kn is greater than 10 [39,40]. The quantity λ_C is taken as a characteristic dimension of a porous system, i.e., the pore diameter, as it is an estimate of the mean confined flight path. Obviously, for arrays of nanocylinders it is not trivial to define a pore diameter. Instead, we derive an explicit formula for λ_C taking Equation 2 and Equation 21.

$$\lambda_C = \frac{4}{\pi} \frac{1}{\sigma d}. \quad (33)$$

λ_B is known from classical molecular kinetics:

$$\lambda_B = \frac{1}{\pi d_m^2 n}, \quad (34)$$

where d_m is the diameter of a molecule. This gives the Knudsen number

$$\text{Kn} = \frac{\sigma d}{4n d_m^2} \quad (35)$$

for an array of randomly distributed vertically aligned nanocylinders. The Knudsen number defined by Equation 4 can be used to verify whether a given system of nanocylinders with areal density σ and mean cylinder diameter d placed in a gas of an arbitrary concentration n and molecular diameter d_m constitutes a confined space for molecular gas transport, and, consequently, whether the kinetic parameters of the gas transport can be estimated using the equations provided in this work.

The aspect ratio of gas transport in nanocylinder arrays

The applicability of our model is further confined by the aspect ratio of gas transport. For nanopores this ratio corresponds straightforwardly to the geometrical aspect ratio of pore length to pore diameter as the transverse molecule flight path is confined by the pore diameter. For nanocylinder arrays the transverse molecule flight path is given by λ_T (Equation 3) and the aspect ratio of gas transport AR_{array} becomes

$$\text{AR}_{\text{array}} := \frac{L}{\lambda_T} = L\sigma d, \quad (36)$$

where L is the cylinder length. In analogy to Clausing [41] we can apply our model for $\text{AR}_{\text{array}} > 10$. For $\text{AR}_{\text{array}} < 10$ a transition to bulk gas diffusion takes place.

Example calculation

We provide an example calculation of Kn and AR_{array} for the system of ALD of titania on VACNTs that appeared to be governed by molecular diffusion in the study of Yazdani and co-workers [17]. In this study the relevant parameters were the following: $d = 10$ nm, $\sigma = 10^{10}$ cm⁻², $L = 100$ μ m, $n = 5 \times 10^{15}$ cm⁻³, $d_m = 1$ nm. Inserting these in Equation 35 and Equation 36, we obtain Kn = 50 and $\text{AR}_{\text{array}} = 100$, both being greater than 10 which lies within the applicability range of our model.

Conclusion

The diffusive transport of dilute gas in an array of vertically aligned system of randomly distributed high-aspect-ratio cylinders of random diameters has been discussed. New formulae have been derived for (i) the mean flight path in space confined by such an array of cylinders, (ii) the mean time of flight, (iii) the impingement rate, (iv) the Knudsen number, and ultimately (v) the diffusion coefficient for such a system using a probabilistic random walk model.

The formulae obtained are of a great assistance in understanding quantitatively the process of gas transport in arrays of vertically aligned cylinders, such as nanotubes or nanowires of various materials. This is crucial for the optimisation of gas-based surface-functionalisation processes of such arrays as well as of the gas sensing performance of such systems, CVD growth of carbon nanotubes or any other fields where gas transport between nanowires or nanotubes is considered.

References

- Chan, C. K.; Peng, H.; Liu, G.; Mcllwraith, K.; Zhang, X. F.; Huggins, R. A.; Cui, Y. *Nat. Nanotechnol.* **2008**, *3*, 31–35. doi:10.1038/nnano.2007.411

2. Song, T.; Xia, J.; Lee, J.-H.; Lee, D. H.; Kwon, M.-S.; Choi, J.-M.; Wu, J.; Doo, S. K.; Chang, H.; Park, W. I.; Zang, D. S.; Kim, H.; Huang, Y.; Hwang, K.-C.; Rogers, J. A.; Paik, U. *Nano Lett.* **2010**, *10*, 1710–1716. doi:10.1021/nl100086e
3. Fan, S.; Chapline, M. G.; Franklin, N. R.; Tomblor, T. W.; Cassell, A. M.; Dai, H. *Science* **1999**, *283*, 512–514. doi:10.1126/science.283.5401.512
4. Kijima, T.; Yoshimura, T.; Uota, M.; Ikeda, T.; Fujikawa, D.; Mouri, S.; Uoyama, S. *Angew. Chem.* **2003**, *116*, 230–234. doi:10.1002/ange.200352630
5. Kasuga, T.; Hiramatsu, M.; Hoson, A.; Sekino, T.; Niihara, K. *Adv. Mater.* **1999**, *11*, 1307–1311. doi:10.1002/(SICI)1521-4095(199910)11:15<1307::AID-ADMA1307>3.0.CO;2-H
6. Xiao, Z. L.; Han, C. Y.; Welp, U.; Wang, H. H.; Kwok, W. K.; Willing, G. A.; Hiller, J. M.; Cook, R. E.; Miller, D. J.; Crabtree, G. W. *Nano Lett.* **2002**, *2*, 1293–1297. doi:10.1021/nl025758q
7. Park, H.-G.; Kim, S.-K.; Song, K.-D.; Kempa, T. J.; Lieber, C. M. Multishell nanowires for next-generation photovoltaics. In *Progress in Electromagnetic Research Symposium (PIERS)*, Shanghai, China, Aug 8–11, 2011; 2016; p 1864. doi:10.1109/PIERS.2016.7734817
8. Wang, C.-C.; Hsueh, Y.-C.; Su, C.-Y.; Kei, C.-C.; Perng, T.-P. *Nanotechnology* **2015**, *26*, 254002. doi:10.1088/0957-4484/26/25/254002
9. Ye, T.; Jun, L.; Kun, L.; Hu, W.; Ping, C.; Ya-Hui, D.; Zheng, C.; Yun-Fei, L.; Hao-Ran, W.; Yu, D. *Org. Electron.* **2017**, *41*, 179–185. doi:10.1016/j.orgel.2016.10.046
10. Lu, X.; Yu, M.; Wang, G.; Zhai, T.; Xie, S.; Ling, Y.; Tong, Y.; Li, Y. *Adv. Mater.* **2013**, *25*, 267–272. doi:10.1002/adma.201203410
11. Lau, K. K. S.; Bico, J.; Teo, K. B. K.; Chhowalla, M.; Amaratunga, G. A. J.; Milne, W. I.; McKinley, G. H.; Gleason, K. K. *Nano Lett.* **2003**, *3*, 1701–1705. doi:10.1021/nl034704t
12. Marichy, C.; Bechelany, M.; Pinna, N. *Adv. Mater.* **2012**, *24*, 1017–1032. doi:10.1002/adma.201104129
13. Qin, Y.; Lee, S.-M.; Pan, A.; Gösele, U.; Knez, M. *Nano Lett.* **2008**, *8*, 114–118. doi:10.1021/nl0721766
14. Zhang, Y.; Guerra-Núñez, C.; Li, M.; Michler, J.; Park, H. G.; Rossell, M. D.; Erni, R.; Utke, I. *Chem. Mater.* **2016**, *28*, 3488–3496. doi:10.1021/acs.chemmater.6b01209
15. Li, J.; Lu, Y.; Ye, Q.; Cinke, M.; Han, J.; Meyyappan, M. *Nano Lett.* **2003**, *3*, 929–933. doi:10.1021/nl034220x
16. Chen, J.; Xu, L.; Li, W.; Gou, X. *Adv. Mater.* **2005**, *17*, 582–586. doi:10.1002/adma.200401101
17. Yazdani, N.; Chawla, V.; Edwards, E.; Wood, V.; Park, H. G.; Utke, I. *Beilstein J. Nanotechnol.* **2014**, *5*, 234–244. doi:10.3762/bjnano.5.25
18. Zhong, G.; Iwasaki, T.; Robertson, J.; Kawarada, H. *J. Phys. Chem. B* **2007**, *111*, 1907–1910. doi:10.1021/jp067776s
19. Xiang, R.; Yang, Z.; Zhang, Q.; Luo, G.; Qian, W.; Wei, F.; Kadowaki, M.; Einarsson, E.; Maruyama, S. *J. Phys. Chem. C* **2008**, *112*, 4892–4896. doi:10.1021/jp710730x
20. Poodt, P.; Cameron, D. C.; Dickey, E.; George, S. M.; Kuznetsov, V.; Parsons, G. N.; Roozeboom, F.; Sundaram, G.; Vermeer, A. *J. Vac. Sci. Technol., A* **2012**, *30*, 10802. doi:10.1116/1.3670745
21. Louchev, O. A.; Laude, T.; Sato, Y.; Kanda, H. *J. Chem. Phys.* **2003**, *118*, 7622. doi:10.1063/1.1562195
22. Zhu, L.; Hess, D. W.; Wong, C.-P. *J. Phys. Chem. B* **2006**, *110*, 5445–5449. doi:10.1021/jp060027q
23. Knudsen, M. *Ann. Phys.* **1909**, *333*, 75–130. doi:10.1002/andp.19093330106
24. Knudsen, M. *Ann. Phys.* **1916**, *353*, 1113–1121. doi:10.1002/andp.19163532409
25. Roy, S.; Raju, R.; Chuang, H. F.; Cruden, B. A.; Meyyappan, M. *J. Appl. Phys.* **2003**, *93*, 4870. doi:10.1063/1.1559936
26. Roy, S.; Cooper, S. M.; Meyyappan, M.; Cruden, B. A. *J. Membr. Sci.* **2005**, *253*, 209–215. doi:10.1016/j.memsci.2004.11.033
27. Gordon, R. G.; Hausmann, D.; Kim, E.; Shepard, J. *Chem. Vap. Deposition* **2003**, *9*, 73–78. doi:10.1002/cvde.200390005
28. Detavernier, C.; Dendooven, J.; Pulinthanathu Sree, S.; Ludwig, K. F.; Martens, J. A. *Chem. Soc. Rev.* **2011**, *40*, 5242. doi:10.1039/c1cs15091j
29. Elam, J. W.; Routkevitch, D.; Mardilovich, P. P.; George, S. M. *Chem. Mater.* **2003**, *15*, 3507–3517. doi:10.1021/cm0303080
30. Elam, J. W. Coatings on High Aspect Ratio Structures. In *Atomic Layer Deposition of Nanostructured Materials*; Pinna, N.; Knez, M., Eds.; Wiley: Weinheim, Germany, 2011; pp 227–249. doi:10.1002/9783527639915.ch10
31. Panda, S. K.; Shin, H. Step Coverage in ALD. In *Atomic Layer Deposition of Nanostructured Materials*; Pinna, N.; Knez, M., Eds.; Wiley: Weinheim, Germany, 2011; pp 23–40. doi:10.1002/9783527639915.ch2
32. Yanguas-Gil, A.; Yang, Y.; Kumar, N.; Abelson, J. R. *J. Vac. Sci. Technol., A* **2009**, *27*, 1235. doi:10.1116/1.3207745
33. Arya, G.; Chang, H.-C.; Maginn, E. J. *Phys. Rev. Lett.* **2003**, *91*, 026102. doi:10.1103/PhysRevLett.91.026102
34. Arya, G.; Chang, H.-C.; Maginn, E. J. *Mol. Simul.* **2003**, *29*, 697–709. doi:10.1080/0892702031000103257
35. Einstein, A. *Investigations on the Theory of the Brownian Movement*; Courier Corporation, 1956.
36. Greenwood, J. *Vacuum* **2002**, *67*, 217–222. doi:10.1016/S0042-207X(02)00173-2
37. Aarik, J.; Aidla, A.; Uustare, T.; Ritala, M.; Leskelä, M. *Appl. Surf. Sci.* **2000**, *161*, 385–395. doi:10.1016/S0169-4332(00)00274-9
38. Tong, T.; Zhao, Y.; Delzeit, L.; Kashani, A.; Meyyappan, M.; Majumdar, A. *IEEE Trans. Compon. Packag. Technol.* **2007**, *30*, 92–100. doi:10.1109/TCAPT.2007.892079
39. Lafferty, J. M., Ed. *Foundations of vacuum science and technology*; Wiley: New York, NY, U.S.A., 1998.
40. Laurendeau, N. M. *Statistical thermodynamics: fundamentals and applications*; Cambridge University Press: New York, NY, U.S.A., 2005. doi:10.1017/CBO9780511815928
41. Clausing, P. *Ann. Phys.* **1932**, *404*, 961–989. doi:10.1002/andp.19324040804

License and Terms

This is an Open Access article under the terms of the Creative Commons Attribution License (<http://creativecommons.org/licenses/by/4.0>), which permits unrestricted use, distribution, and reproduction in any medium, provided the original work is properly cited.

The license is subject to the *Beilstein Journal of Nanotechnology* terms and conditions: (<http://www.beilstein-journals.org/bjnano>)

The definitive version of this article is the electronic one which can be found at:
[doi:10.3762/bjnano.8.7](https://doi.org/10.3762/bjnano.8.7)